Redox Biology 22 (2019) 101148

Contents lists available at ScienceDirect

Redox Biology

journal homepage: www.elsevier.com/locate/redox

Research Paper

Double deletion of PINK1 and Parkin impairs hepatic mitophagy and exacerbates acetaminophen-induced liver injury in mice

Hua Wang[a,b], Hong-Min Ni[b], Xiaojuan Chao[b], Xiaowen Ma[b], Yssa Ann Rodriguez[c], Hemantkumar Chavan[b], Shaogui Wang[b], Partha Krishnamurthy[b], Rick Dobrowsky[c], De-Xiang Xu[a], Hartmut Jaeschke[b], Wen-Xing Ding[b,*]

[a] Department of Toxicology, School of Public Health, Anhui Medical University, Hefei City, Anhui Province, 230032, China
[b] Department of Pharmacology, Toxicology and Therapeutics, University of Kansas Medical Center, Kansas City, KS, 66160, USA
[c] Department of Pharmacology and Toxicology, University of Kansas, Lawrence, KS, 66045, USA

ARTICLE INFO

Keywords:
Autophagy
Cell death
Drug
Hepatotoxicity
Mitochondria

ABSTRACT

Mitochondria damage plays a critical role in acetaminophen (APAP)-induced necrosis and liver injury. Cells can adapt and protect themselves by removing damaged mitochondria via mitophagy. PINK1-Parkin pathway is one of the major pathways that regulate mitophagy but its role in APAP-induced liver injury is still elusive. We investigated the role of PINK1-Parkin pathway in hepatocyte mitophagy in APAP-induced liver injury in mice. Wild-type (WT), PINK1 knockout (KO), Parkin KO, and PINK1 and Parkin double KO (DKO) mice were treated with APAP for different time points. Liver injury was determined by measuring serum alanine aminotransferase (ALT) activity, H&E staining as well as TUNEL staining of liver tissues. Tandem fluorescent-tagged inner mitochondrial membrane protein Cox8 (Cox8-GFP-mCherry) can be used to monitor mitophagy based on different pH stability of GFP and mCherry fluorescent proteins. We overexpressed Cox8-GFP-mCherry in mouse livers via tail vein injection of an adenovirus Cox8-GFP-mCherry. Mitophagy was assessed by confocal microscopy for Cox8-GFP-mCherry puncta, electron microscopy (EM) analysis for mitophagosomes and western blot analysis for mitochondrial proteins. Parkin KO and PINK1 KO mice improved the survival after treatment with APAP although the serum levels of ALT were not significantly different among PINK1 KO, Parkin KO and WT mice. We only found mild defects of mitophagy in PINK1 KO or Parkin KO mice after APAP, and improved survival in PINK1 KO and Parkin KO mice could be due to other functions of PINK1 and Parkin independent of mitophagy. In contrast, APAP-induced mitophagy was significantly impaired in PINK1-Parkin DKO mice. PINK1-Parkin DKO mice had further elevated serum levels of ALT and increased mortality after APAP administration. In conclusion, our results demonstrated that PINK1-Parkin signaling pathway plays a critical role in APAP-induced mitophagy and liver injury.

1. Introduction

Acetaminophen (APAP) overdose-induced liver injury remains the most frequent cause of acute liver failure in the US and other western countries. Decades of work from many laboratories have led to the enriched understanding of APAP overdose-induced liver injury [1–6]. Following APAP overdose, hepatic levels of *N*-acetyl-*p*-benzoquinone imine (NAPQI) increased via the metabolism mediated by cytochrome P450 2E1 (Cyp2e1) and Cyp1a2. Excessive production of NAPQI then depletes intracellular and mitochondrial glutathione (GSH) within the liver whereas the remaining NAPQI forms covalent links with cellular proteins to form APAP protein adducts (APAP-AD). Some of the proteins are mitochondrial proteins resulting in mitochondrial damage and necrotic cell death in the liver [6].

Abbreviations: ALT, alanine aminotransferase; APAP, acetaminophen; APAP-DA, APAP-protein adducts; Cyp2e1, cytochrome P450 2E1; DKO, double knockout; GSH, glutathione; H&E, hematoxylin and eosin; JNK, c-jun N-terminal kinase; KO, knockout; LC3, microtubule-associated light chain 3; NAPQI, *N*-acetyl-*p*-benzoquinone imine; PINK1, phosphatase and tensin homolog (PTEN)-induced kinase 1; TUNEL, terminal dUTP nick-end labeling; OCR, oxygen consumption rate; VDAC, voltage-dependent anion channel; WT, Wild-type

* Corresponding author. Department of Pharmacology, Toxicology and Therapeutics, University of Kansas Medical Center, MS 1018, 3901 Rainbow Blvd., Kansas City, KS, 66160, USA.
E-mail address: wxding@kumc.edu (W.-X. Ding).

https://doi.org/10.1016/j.redox.2019.101148
Received 15 December 2018; Received in revised form 16 February 2019; Accepted 17 February 2019
Available online 20 February 2019

We previously demonstrated that autophagy protects against APAP-induced liver injury via removal of APAP-AD and damaged mitochondria [7–9]. Autophagic removal of damaged mitochondria is mediated by a selective autophagy process termed as mitophagy. Among the mitophagy signaling pathways, phosphatase and tensin homolog (PTEN)-induced kinase 1 (PINK1)-Parkin pathway is so far the best characterized [10,11]. In healthy mitochondria, PINK1 is cleaved by the inner mitochondrial membrane protease PARL and the truncated form of PINK1 is released into the cytosol for N-end recognition and degraded by the proteasome [12]. In damaged and depolarized mitochondria, PINK1 is stabilized on the outer mitochondrial membrane [13–15]. Parkin is an E3 ligase that generally sits in the cytoplasm under normal conditions. Stabilized PINK1 on dysfunctional mitochondria phosphorylates Ser65 on ubiquitin and Ser65 within Parkin's UBL domain that not only leads to the recruitment of Parkin to mitochondria but also enhances Parkin E3 ligase activity resulting in outer mitochondrial membrane protein ubiquitination [16]. In contrast, PTEN-L, a newly identified isoform of PTEN, negatively regulates mitophagy by dephosphorylating ubiquitin via its protein phosphatase activity [17]. Ubiquitinated mitochondria then further recruit autophagy receptor proteins such as NDP52, optineurin (OPTN) and SQSTM1/p62 (hereafter referred to as p62) to mitochondria to trigger the selective mitophagy [10,11,18,19]. Most published data from earlier genetic *Drosophila* and cultured mammalian cell models suggest a linear PINK1-Parkin mitophagy pathway, which places PINK1 upstream of Parkin [15,20]. However, recent evidence suggests a new model that PINK1 alone can also induce mitophagy independent of Parkin via directly recruit NDP52 and OPTN, two other mitophagy receptor proteins, to mitochondria [21].

Although we now understand extensively the molecular details by which PINK1-Parkin regulates mitophagy, most of the known mechanisms are derived from cell culture studies that overexpress exogenous Parkin. Due to the lack of reliable quantitative mitophagy assays, relatively few studies were conducted to determine the role of PINK1-Parkin in mitophagy under pathophysiologically relevant *in vivo* conditions. We recently demonstrated that APAP increases Parkin translocation to mitochondria, which is associated with increased ubiquitination of mitochondrial proteins and mitophagy in mouse livers [8]. These data imply that Parkin-mediated mitophagy may be protective against APAP-induced liver injury by removing damaged mitochondria. Unexpectedly, we also found that mitophagy still occurs in APAP-treated Parkin knockout (KO) mouse livers and that Parkin KO mice are resistant to APAP-induced liver injury [11], suggesting other compensatory mechanisms may be activated to induce mitophagy in Parkin KO mouse livers. The aim of the present study was to determine the role of PINK1 and Parkin in APAP-induced mitophagy and liver injury, and whether PINK1-mediated mitophagy would serve as a compensatory mechanism in the absence of Parkin in APAP-treated mouse livers. To achieve a more reliable quantitative measure of mitophagy in mouse livers, we generated an adenovirus vector that carries a mitochondrial inner membrane-targeted tandem GFP-mCherry fusion protein. To determine the possible reciprocal compensatory role of PINK1 and Parkin in APAP-induced mitophagy and liver injury, we also generated PINK1 and Parkin double KO (DKO) mice. We found that APAP-induced mitophagy was significantly blunted in the PINK1 and Parkin DKO mice. As a result, PINK1 and Parkin DKO mice had more severe liver damage and increased mortality compared with either wild-type (WT) mice or single PINK1 KO or Parkin KO mice after APAP.

2. Materials and methods

2.1. Antibodies and reagents

The following antibodies were used for western blot analysis: Parkin (Santa-Cruz, SC-32282), Ubiquitin (Santa Cruz, SC-8017), p62 (Abnova, H00008878-M01), β-Actin (Sigma, A5441), Cyp2e1 (Abcam, ab19140), phosphorylated JNK (4668S), JNK (BD, 554285), Oxphos rodent antibody cocktail (Abcam, ab110413), and voltage-dependent anion channel (VDAC) (Calbiochem, 529534). The APAP-adduct antibody was a gift from Dr. Lance Pohl (NIH) [22]. Horseradish peroxidase-conjugated antibodies were from Jackson ImmunoResearch Lab. Adenovirus (Ad) Cox8-GFP-mCherry was produced in collaboration with Vector Biolabs (Malvern, PA). In situ cell death detection kit (Cat# 11684809910) was purchased from Roche. The kit for alanine aminotransferase (ALT) assay was purchased from Pointe Scientific (A7526-450). APAP and other chemicals were either purchased from Sigma-Aldrich or Thermo Fisher Scientific.

2.2. Animal experiments

WT C57BL/6J, PINK1 KO (stock# 017946) and Parkin KO (Stock# 006582) were purchased from the Jackson Laboratory. PINK1 and Parkin DKO mice were generated by crossing PINK1 KO mice with Parkin KO mice. Atg5 Flox/Flox (Atg5 F/F) mice (C57BL/6/129) were generated by Dr. N. Mizushima and were backcrossed with C57BL/6J for another 10 generations before further crossing them with Albumin-Cre mice (Alb-Cre, C57BL/6) (Jackson Laboratory) as described previously [23].

Male 8 to 12 week-old mice were treated with APAP (500 mg/kg) or saline by intraperitoneal injection. Afterwards, mice were euthanized at 2, 6, or 24 h. For the overexpression of Cox8-GFP-mCherry experiments, mice were first given adenovirus (Ad)-Cox8-GFP-mCherry (5×10^8 PFU/mouse, i.v) for 5 days followed by APAP (500 mg/kg) for 6 h. All animals received humane care, and all protocols were approved by the Institutional Animal Care and Use Committee at the University of Kansas Medical Center.

Mouse livers and blood were collected. Hepatic function was evaluated by measuring serum alanine aminotransferase (ALT) activities. Formalin-fixed liver tissues were embedded in paraffin and cut into 5-μm sections before staining with hematoxylin and eosin (H&E) or terminal dUTP nick-end labeling (TUNEL).

2.3. Confocal and electron microscopy for mitophagy in vitro and in vivo

Cryo-liver sections from saline and APAP-treated mice that overexpressed Cox8-GFP-mCherry were further stained with Hoechst33342 (1 μg/ml) followed by confocal microscopy using a Leica confocal microscope. Images were acquired digitally using an oil lens at 40×. More than 5 images were taken from one mouse liver section and the number of red-only puncta in each cell was counted in more than 18 cells per mouse from 3 different mice. For the electron microscopy (EM), liver tissues were fixed with 2% glutaraldehyde in 0.1 M phosphate buffer (pH 7.4) followed by 1% OsO_4. After dehydration, thin sections were stained with uranyl acetate and lead citrate for observation under a JEM 1016CX electron microscope. The number of autophagosomes that enveloped with mitochondria (mitophagosomes) was counted and normalized to the cytosolic areas using a SPOT software (SPOT Imaging). More than 10 different cells were analyzed in each group. Murine hepatocytes were isolated according to the methods described previously [24]. Cells were cultured in Williams Medium E and maintained in a 37 °C incubator with 5% CO_2. To examine mitophagy in primary hepatocytes, primary hepatocytes were seeded in a 12 well-plate (2×10^5 in each well) and infected with adenovirus-Cox8-GFP-mCherry (5 moi) for 24 h. Cells were fixed with 4% paraformaldehyde in phosphate buffered saline (PBS) and kept at 4 °C for microscopy. Fluorescence images were acquired under a Nikon Eclipse 200 fluorescence microscope with MetaMorph software.

2.4. Western blot analysis

Total liver lysates were prepared using RIPA buffer (1% NP40, 0.5% sodium deoxycholate, 0.1% sodium dodecyl (lauryl) sulfate). Heavy

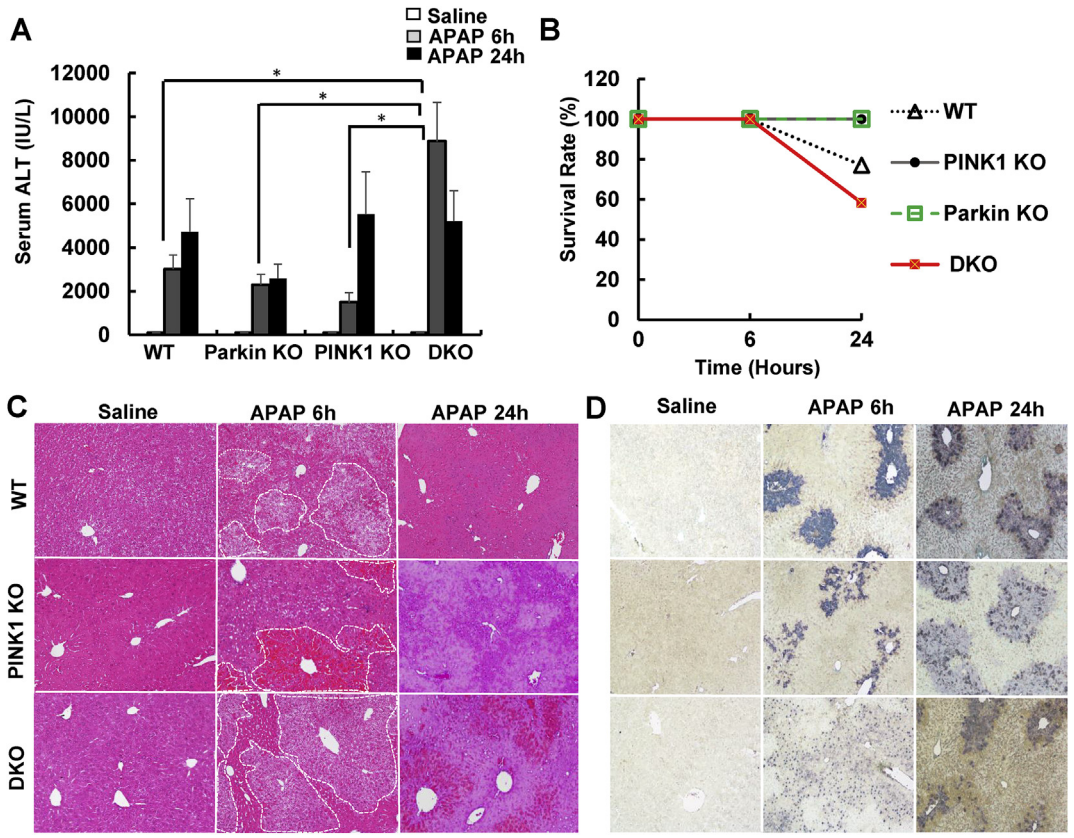

Fig. 1. PINK1 and Parkin DKO mice are more susceptible to APAP-induced liver injury. Male WT, Parkin KO, PINK1 KO, PINK1 and Parkin DKO (C57BL/6J) mice were treated with APAP (500 mg/kg, i.p.) or saline for 6 and 24 h. (**A**) Serum ALT level. Data are shown as mean ± *SE* (n = 5–13). *$p < 0.05$, One-way ANOVA analysis. (**B**) Mouse survival rate after APAP treatment (n = 7–15). (**C**) Representative images from H&E staining and (**D**) TUNEL staining in mouse livers. Dot line-circled areas represent necrotic areas.

membrane (HM) fractions mainly enriched with mitochondria and cytosolic fractions were prepared as described previously [25]. Briefly, liver tissues were homogenized in HIM buffer (200 mM mannitol, 70 mM sucrose, 5 mM Hepes, 0.5 mM EGTA (pH 7.5) containing 1% protease inhibitors) using a dounce homogenizer. Homogenates were centrifuged at 1000 × *g* to remove debris, and the supernatant was centrifuged at 10,000 × *g* for 10 min to separate HM and cytosolic fractions. The supernatant was kept as the cytosolic fraction, and the pellet containing the HM fraction was further washed by centrifugation and re-suspended in HIM buffer. To determine the levels of mitochondrial oxidative phosphorylation (OXPHOS) proteins, 30 μg protein were mixed with the loading sample buffer at room temperature without heat boiling. Protein (30 μg) was separated by a 12%–15% SDS-PAGE gel before transfer to a PVDF membrane. Membranes were probed using indicated primary and secondary antibodies and developed with SuperSignal West Pico chemiluminescent substrate (Pierce, 34080) and high sensitivity for chemiluminescent substrate (Millipore, WBKLS0500).

2.5. Glutathione (GSH) assay and APAP-protein adducts measurement

GSH levels in mouse livers were detected using a modified Tietze assay [26]. Briefly, liver tissues were homogenized in sulfosalicylic acid (3%) followed by centrifugation and dilution in potassium phosphate buffer. Samples were then subjected to a cycling reaction using glutathione reductase and dithionitrobenzoic acid, and GSH levels were determined by spectrophotometry [27]. The levels of serum and liver APAP-adducts were determined by western blot analysis using an anti-APAP-adduct antibody as we described previously [7].

2.6. Measurement of mitochondria bioenergetics

This was performed as we recently reported [28]. Briefly, livers were homogenized in mitochondria isolation buffer (70 mM sucrose, 210 mM mannitol, 5 mM HEPES, 1 mM EGTA and 0.5% (w/v) fatty acid-free BSA; pH 7.2). Homogenates were centrifuged twice at 1000 × *g* for 10 min at 4 °C and the supernatants were centrifuged once at 8000 × *g* for 10 min at 4 °C. The mitochondrial pellets were suspended in the isolation buffer and total proteins were determined using BCA protein assay. All mitochondrial respiration assays were performed using an XF24x3 Extracellular Flux Analyzer by Seahorse Bioscience (North Billerica, Massachusetts). Mitochondria from 2 to 3 mice/group were pooled and the assays were done in triplicate. Isolated liver mitochondria were suspended in cold mitochondrial assay solution (1 × MAS: 70 mM sucrose, 220 mM mannitol, 10 mM KH_2PO_4, 5 mM $MgCl_2$, 2 mM HEPES, 1 mM EGTA and 0.2% (w/v) fatty acid-free BSA, pH 7.2 at 37 °C) containing substrate (10 mM succinate + 2 μM rotenone) to a final concentration of 0.2 mg/ml protein, and 50 μl of this mitochondrial suspension was plated to each well (except for background correction wells). The plate was centrifuged at 2000 × *g* for 20 min at 4 °C and 450 μl of 1 × MAS-substrate solution was added to each well. The sensor cartridge was loaded with port A, 40 mM ADP (4 mM final); port B, 25 μg/ml oligomycin (2.5 μg/ml final); port C, 40 μM FCCP (4 μM final); and port D, 40 μM antimycin A (4 μM final) to measure the bio-energetic profile. The plate was pre-warmed to 37 °C and transferred to the XF24 instrument. The respiration was measured in a coupled state with substrate present (basal respiration), followed by State 3 (phosphorylating respiration, in the presence of ADP and substrate), State 4o (leak state induced with the addition of oligomycin - inhibitor of ATP synthase), and then maximal uncoupler (FCCP)-

stimulated respiration (State 3u). At the end, antimycin A (complex III inhibitor) is added to inhibit mitochondrial respiration completely.

2.7. Statistical analysis

All analyses were performed using Student's *t*-test or one-way ANOVA analysis where appropriate. Difference was considered significant at *P* value less than 0.05.

3. Results

3.1. Double deletion of PINK1 and Parkin exacerbates APAP-induced liver injury and mortality in mice

Similar to Parkin KO mice that we reported previously [8], we found that PINK1 KO mice had decreased serum ALT levels at 6 h compared with WT mice after APAP. After 24 h treatment with APAP, levels of ALT in Parkin KO mice remained as low as in 6 h, but the serum ALT levels increased slightly in both WT and PINK1 KO mice. In contrast, DKO mice had significantly higher serum levels of ALT than WT mice or either PINK1 or Parkin single KO mice at 6 h after APAP treatment (Fig. 1A). We found that the mortality of DKO mice doubled compared with WT mice (41.7% vs 23.1%) whereas all the PINK1 KO and Parkin KO mice survived after APAP treatment for 24 h (Fig. 1B). Because we could only assess the ALT values in the survived DKO mice, which may explain why the ALT levels were comparable among the WT, PINK1 KO and DKO mice at 24 h. Consistent with the serum ALT and mouse survival data, liver H&E and TUNEL staining revealed increased necrotic areas in the DKO mice compared with PINK1 KO and WT mice after APAP treatment for 6 and 24 h (Fig. 1C&D). Taken together, these findings indicate that PINK1 and Parkin DKO mice are more susceptible to APAP-induced liver injury and mortality in mice. Increased liver injury in PINK1 KO but not in Parkin KO mice after APAP treatment for 24 h also suggests that PINK1 may have additional functions in addition to serving as a linear upstream regulator of Parkin-mediated mitophagy.

3.2. Delayed glutathione (GSH) recovery in PINK1 and Parkin DKO mice after APAP

We found that the hepatic levels of Cyp2e1 were comparable among all these different genotypes of mice (Fig. 2A). Consistent with the Cyp2e1 data, we found that hepatic GSH levels decreased markedly to almost the same levels among WT, PINK1 KO, Parkin KO and DKO mice after 2 h of APAP treatment. Western blot analysis revealed completely deletion of Parkin protein in Parkin KO and DKO mice. Using the current commercial PINK1 antibody, we could not detect PINK1 at the basal or after APAP treatment in mouse livers. However, we have confirmed the deletion of PINK1 by PCR genotyping and qRT-PCR for hepatic PINK1 mRNA expression (data not shown). These data suggest that PINK1 KO, Parkin KO and DKO mice may not affect the bioactivation and metabolism of APAP. However, while WT, PINK1 KO and Parkin KO mice had the same recovery rate of hepatic GSH, the levels of hepatic GSH remained low in DKO mice after APAP treatment for 6 h (Fig. 2B). Together these results indicate that PINK1 KO as well as PINK1 and Parkin DKO mice do not affect APAP metabolism and DKO mice have delayed hepatic GSH recovery.

3.3. Decreased hepatic levels of mitochondrial ubiquitination and p62 translocation in PINK1 and Parkin DKO mice after APAP treatment

Parkin recruitment to mitochondria and subsequent mitochondrial ubiquitination is a crucial process to trigger mitophagy [29]. We found that APAP increased the levels of mitochondrial Parkin after APAP treatment in WT mice, which is in agreement with our previous report [8]. However, APAP did not increase mitochondrial Parkin translocation in PINK1 KO mice, suggesting that PINK1 is required for Parkin mitochondrial translocation in mouse livers (Fig. 3A), which is consistent with the findings in various cell culture studies [14,15]. Compared with the saline treatment group, APAP treatment markedly increased mitochondrial ubiquitination in WT, Pink1 KO and Parkin KO mice, which were blunted in PINK1 and Parkin DKO mice. The basal level of mitochondrial ubiquitination was relatively higher in PINK1 KO mice (saline-treated group), which only slightly increased after APAP treatment. The levels of mitochondrial p62 increased in WT, PINK1 KO and Parkin KO mice but not in DKO mice after APAP treatment (Fig. 3B). Importantly, when we placed isolated mitochondria from all four different genotype mice after APAP treatment on the same blot for the direct comparison, we found that mitochondrial ubiquitination occurred in WT, PINK1 KO and Parkin KO mice whereas only minimal levels of mitochondrial ubiquitination were detected in DKO mice (Fig. 3C). Similarly, APAP-induced levels of p62 mitochondrial translocation slightly decreased in PINK1 KO and Parkin KO mice but markedly decreased in PINK1 and Parkin DKO mice compared with WT mice. These data suggest that single genetic deletion of either PINK1 or Parkin is not sufficient to significantly blunt APAP-induced mitochondrial ubiquitination and p62 translocation. The markedly decreased mitochondrial ubiquitination and p62 translocation in APAP-treated DKO mice may imply that PINK1 could compensate for the loss of Parkin and vice versa that Parkin could compensate for the loss of PINK1 at least partially in regulating APAP-induced mitochondria ubiquitination and p62 translocation and subsequent mitophagy.

3.4. Impaired hepatic mitophagy and increased mitochondrial dysfunction in APAP-treated PINK1 and Parkin DKO mice

To better determine mitophagy after APAP treatment in hepatocytes, we developed a novel tandem Cox8-GFP-mCherry fusion protein

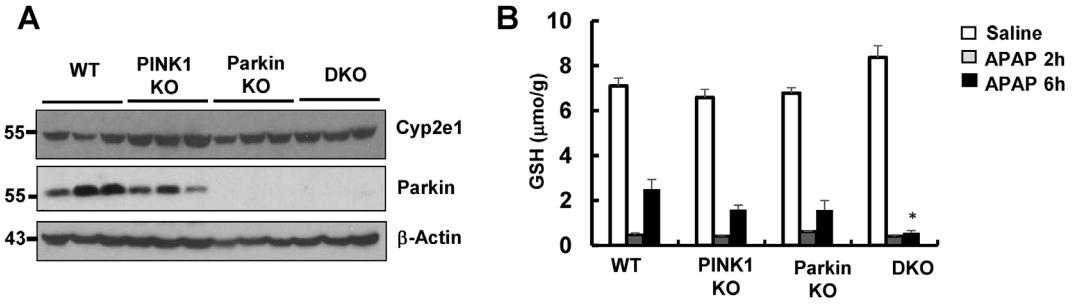

Fig. 2. Delayed glutathione (GSH) recovery in PINK1 and Parkin DKO mice after APAP treatment. Male WT, Parkin KO, PINK1 KO, PINK1 and Parkin DKO (C57BL/6J) mice were treated with APAP (500 mg/kg, i.p.) or saline for 2 and 6 h. (**A**) Total liver lysates from mice that were treated with APAP (6 h) and saline were subjected to western blot analysis. (**B**) Hepatic GSH levels were measured. Data are presented as mean ± SE (n = 3). $^{*}p < 0.05$ as compared with WT mice. One-way ANOVA analysis.

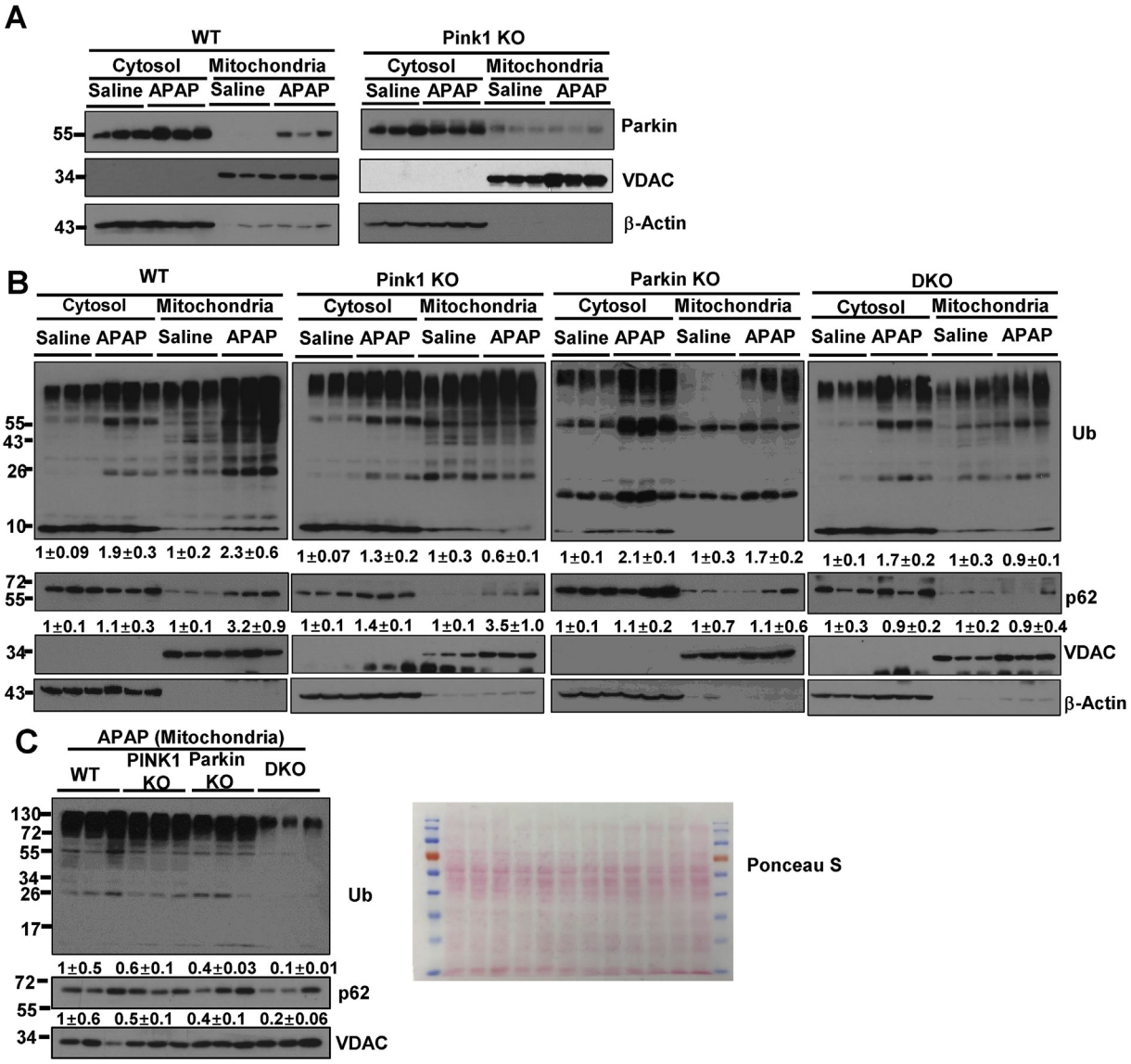

Fig. 3. Decreased hepatic levels of mitochondrial ubiquitination and p62 translocation in PINK1 and Parkin DKO mice after APAP treatment. Male WT, Parkin KO, PINK1 KO, PINK1 and Parkin DKO (C57BL/6J) mice were treated with APAP (500 mg/kg, i.p.) or saline for 6 h. (A) Liver cytosolic and mitochondrial fractions were isolated and subjected to western blot analysis for Parkin and (B) for ubiquitin and p62. β-Actin and VDAC were used as loading controls for cytosol and mitochondria, respectively. Densitometry analysis were performed for ubiquitin (ub) and p62 and values were normalized either to β-Actin or VDAC. Data are means ± SE (n = 3 mice). (C) Mitochondrial fractions from APAP-treated WT, Parkin KO, PINK1 KO and DKO mice were subjected to western blot analysis. Densitometry analysis were performed for ubiquitin (ub) and p62 and values were normalized to VDAC. Data are means ± SE (n = 3 mice). A photograph of Ponceau S red staining membrane serves as a loading control.

that targets the mitochondrial inner membrane in hepatocytes using an adenovirus-Cox8-GFP-mCherry. In this assay, mCherry fluorescence is more stable in acidic compartments whereas GFP fluorescence is rapidly quenched, which is similar to the tandem mCherry-GFP-LC3 that is widely used to monitor autophagic flux [30]. Accordingly, once mitochondria are delivered to autolysosomes via the fusion of lysosomes with autophagosomes that have enveloped mitochondria, the numbers of red only (mCherry) puncta increased. Failure to deliver mitochondria to acidic autolysosomes or suppression of lysosomal degradation (i.e., increase lysosomal pH) would decrease the number of red mitochondria. We first validated the use of Cox8-GFP-mCherry to monitor mitophagy in primary cultured hepatocytes that were isolated from WT and liver-specific Atg5 KO mice. We found that Cox8-GFP-mCherry showed spherical or tubular like typical mitochondrial structure in primary mouse hepatocytes from WT and Atg5 KO mice (Fig. 4A), suggesting successful overexpression and targeting of Cox8-GFP-mCherry to mitochondria in hepatocytes. We found many red only (mCherry only) puncta in WT hepatocytes, which reflects the basal level mitophagy in primary cultured hepatocytes. In contrast, Cox8-GFP-mCherry displayed almost exclusively yellow color mitochondria in Atg5 KO hepatocytes, suggesting a marked decrease of mitophagy (Fig. 4). These data indicate that Cox8-GFP-mCherry can be used to specifically monitor mitophagy in hepatocytes. To further determine mitophagy in mouse livers using Cox8-GFP-mCherry after APAP, we overexpressed Cox8-GFP-mCherry in mouse livers by tail vein injection of Ad-Cox8-GFP-mCherry. Similar to the primary cultured hepatocytes, we also found Cox8-GFP-mCherry displayed spherical or tubular like typical mitochondrial structure in hepatocytes of mouse livers. In saline-treated WT, PINK1 KO and Parkin KO mouse livers, we found approximately average 18 red-only puncta per hepatocyte, which may reflect the basal mitophagy in the livers of these mice. In contrast, there were approximately 12 red-only puncta per hepatocytes in saline-

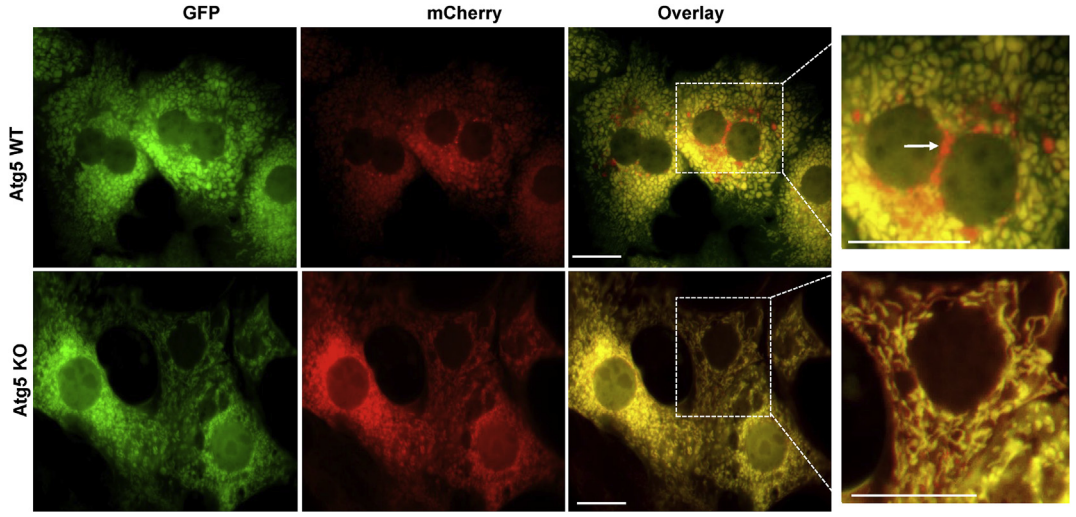

Fig. 4. Cox8-GFP-mCherry assay reveals that Atg5 KO hepatocyte have decreased mitophagy. Primary hepatocytes were isolated from WT and liver-specific Atg5 KO mice and infected with Ad-Cox8-GFP-mCherry (5 moi) for 24 h. Cells were fixed and followed by fluorescence microscopy. Representative images are shown. Right panels are enlarged photographs from the boxed areas. Arrow denotes the red-only puncta. Bar: 10 μm.

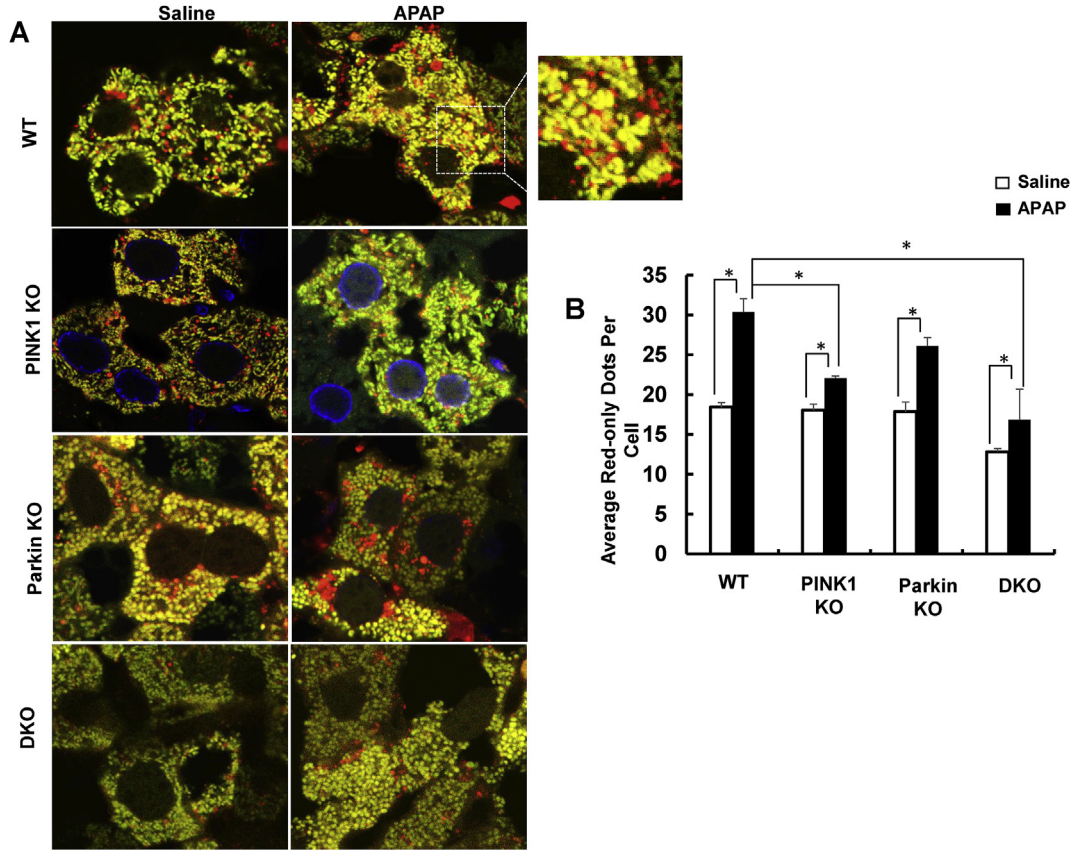

Fig. 5. Decreased red puncta numbers of Cox8-GFP-mCherry in APAP-treated PINK1 and Parkin DKO mouse livers. Male WT, PINK1 KO, Parkin KO, and PINK1 and Parkin DKO (C57BL/6J) mice were injected with Ad-Cox8-GFP-mCherry (5×10^8 PFU/mouse, i.v) for 5 days followed by APAP (500 mg/kg) for 6 h. Cryo-liver sections were subjected to confocal microscopy. (**A**) Representative confocal microscopy images of Cox8-GFP-mCherry of mouse livers. The right panel is from the boxed area of the next panel. Arrows denote red puncta. Scale Bar: 10 μm. (**B**) Average number of red-only puncta per hepatocyte. Data are means ± SE (n = 3 mice). Eighteen to thirty-two hepatocytes were counted in each mouse. *p < 0.05; One-way ANOVA analysis.

treated PINK1 and Parkin DKO mouse livers. APAP treatment increased the number of red-only puncta significantly compared with saline-treated mice, which was significantly blunted in PINK1 and Parkin DKO mice (Fig. 5A&B).

To further determine APAP-induced mitophagy in WT and PINK1 and Parkin DKO mice, we compared and quantified the number of autophagosomes and lysosomes containing mitochondria (hereafter referred to as mitophagosomes) by EM analysis. We found that APAP-treatment increased the number of hepatic mitophagosomes in WT, PINK1 KO, and PINK1 and Parkin DKO mice compared with their respective saline-treated control mice. However, the number of mitophagosomes is much lower in APAP-treated DKO mice than in WT and

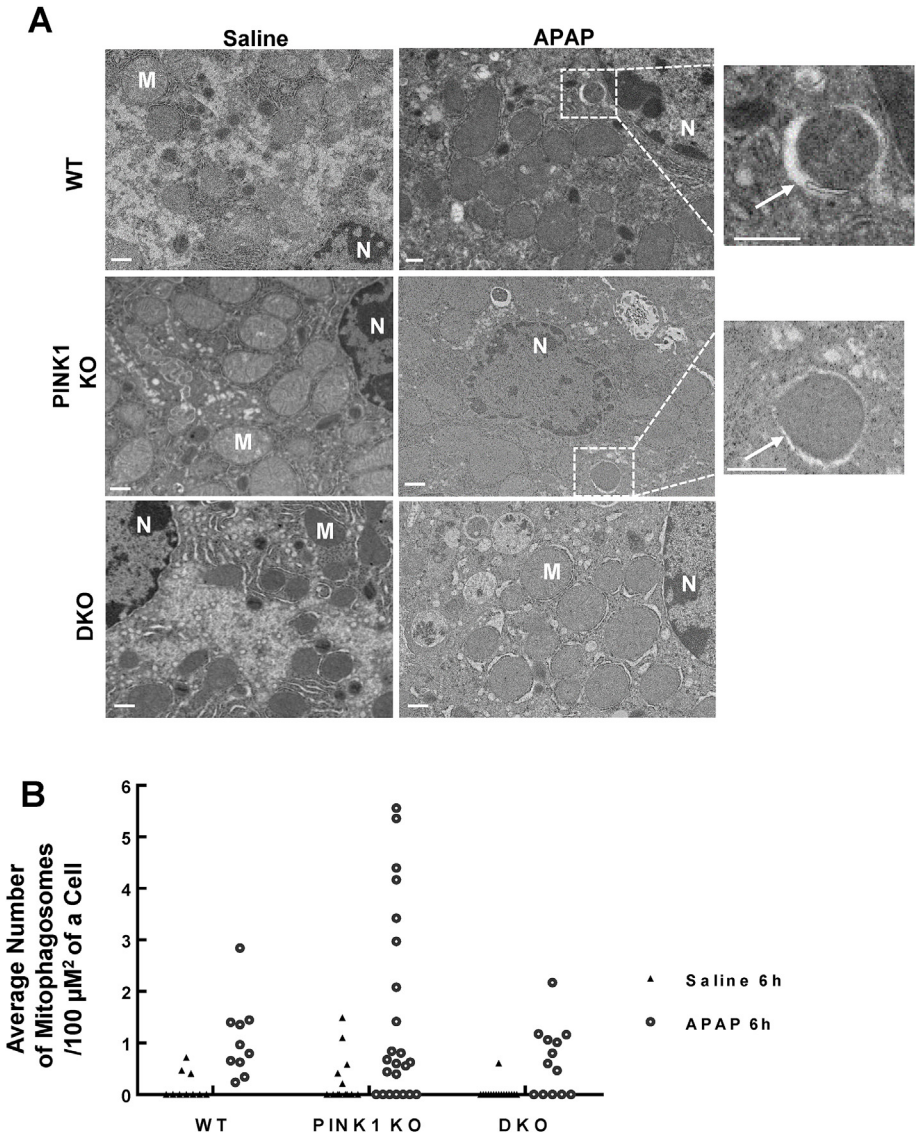

Fig. 6. Impaired hepatic mitophagy in APAP-treated PINK1/Parkin DKO mice. Male WT, PINK1 KO, PINK1 and Parkin DKO (C57BL/6J) mice were treated with APAP (500 mg/kg, i.p.) or saline for 6 h. (**A**) Representative EM images from WT, PINK1 KO, Parkin KO, and PINK1/Parkin DKO mouse livers are shown. Right panels are enlarged photographs from the boxed areas in the left panels. Arrows denote for the mitophagosomes. M = mitochondria, N = nucleus. Bar = 500 nm. (**B**) Quantification of the number of mitophagosomes from EM. Data shown are dot plot of the mitophagosomes that contain mitochondria from at least 10 images of the mouse liver.

PINK1 KO mice (Fig. 6A&B). While these changes did not reach statistical significance due to the variations, these data confirmed that the structures of autophagosomes that enveloped with mitochondria (mitophagosomes) could be detected in APAP-treated mouse livers regardless of the presence of PINK1 or Parkin. However, the very low levels of mitophagosomes from the EM studies together with the low levels of red-only puncta in PINK1 and Parkin DKO mice from the Cox8-GFP-mCherry assay, suggesting that APAP-induced mitophagy is largely dependent on PINK1-Parkin pathway in the mouse livers.

3.5. Elevated levels of hepatic mitochondrial proteins and decreased mitochondrial respiration in APAP-treated PINK1 and Parkin DKO mice

We next determined the levels of several mitochondrial oxidative phosphorylation (OXPHOS) proteins (consist of complex I, II, III, IV and V) after APAP treatment. As can be seen, APAP treatment led to an overall decrease of OXPHOS complex proteins at 6 and 24 h in WT mice. In Parkin KO mice, the levels of the OXPHOS complex proteins remained unchanged after APAP treatment for 6 h but the levels of complex I significantly decreased after APAP treatment for 24 h compared to the saline-treated group. In contrast, after APAP treatment, the levels of the OXPHOS complex proteins remained almost unchanged at both 6 and 24 h in PINK1 KO and DKO mice except that the level of complex I deceased 50% in PINK1 KO compared with the saline control group (Fig. 7A&B).

To make a direct comparison of mitochondrial proteins after APAP, we placed proteins from all saline-treated and APAP-treated different genotype of mice on the same blot. The basal levels of OXPHOS were not significantly different among the different genotype mice except that the levels of complex I were higher in PINK1 KO, Parkin KO and DKO mice compared with the WT mice. After APAP treatment, levels of OXPHOS protein were also comparable among the different genotype mice but the levels of complex IV were significantly higher in DKO mice compared with the other mice (Fig. 7C&D). Moreover, when isolated mitochondria from APAP-treated different genotype of mice were used to measure the mitochondrial oxygen consumption rate (OCR) using Seahorse XF24x3 extracellular flux analyzer, we found no difference in either basal respiration, ATP-synthesizing respiration (state III) or maximum respiratory capacity induced by uncoupling with FCCP (state 3u) among WT, PINK1 KO and Parkin KO mice. In contrast, all the different states of mitochondrial respiration decreased significantly in DKO mice compared with WT, PINK1 KO and Parkin KO mice either treated with saline or APAP (Fig. 7E). It should be noted that the OCR change patterns remained the same when the values of antimycin were subtracted (data not shown). It has been generally thought that the outer mitochondrial membrane proteins are largely degraded via the

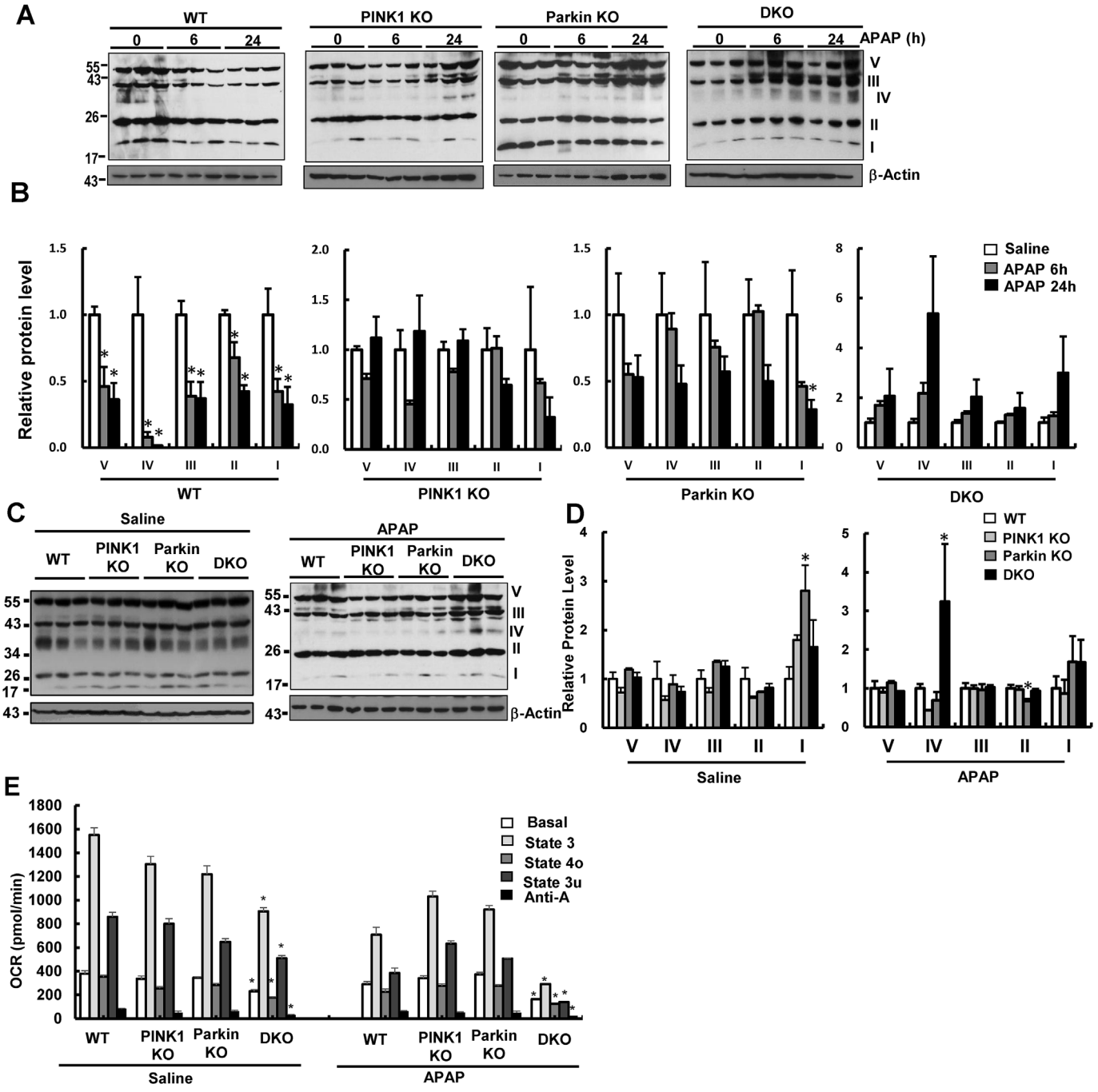

Fig. 7. Inner mitochondrial membrane proteins are not degraded but mitochondrial respiration decreased in APAP-treated PINK1 and Parkin DKO mice. Male WT, PINK1 KO, Parkin KO, PINK1 and Parkin DKO (C57BL/6J) mice were treated with APAP (500 mg/kg, i.p.) or saline for 6 and 24 h. (**A**) Total liver lysates were subjected to western blot analysis. (**B**) Densitometry analysis of (**A**). Data are means ± SE (n = 3). (**C**) Total liver lysates from saline-treated and APAP-treated WT, PINK1 KO, Parkin KO, PINK1 and Parkin DKO mice were subjected to western blot analysis. (**D**) Densitometry analysis of (**C**). Data are means ± SE (n = 3). *p < 0.05 One-way ANOVA analysis. (**E**) Isolated hepatic mitochondria were subjected to the analysis of mitochondrial bioenergetics using Seahorse XF24x3 analyzer. All results are expressed as means ± SE (n = 3) and experiments were repeated more than 3 times. *p < 0.05 Student t-test.

ubiquitin proteasome system whereas the inner mitochondrial membrane proteins are degraded via autophagy [29,31]. We found that the levels of Mfn1, Tom20 and VDAC, three outer mitochondrial membrane proteins, markedly decreased in WT mice after APAP treatment. In contrast, no degradation of Tom20 and VDAC was observed in PINK1 KO, Parkin KO and DKO mice after APAP treatment. The levels of Mfn1 only decreased in PINK1 KO and Parkin KO mice after prolonged treatment with APAP for 24 h but levels of Mfn1 remained unchanged in DKO mice after APAP treatment (Fig. 8 A&B). Together, these data suggest that PINK1 and Parkin DKO mice have generally less mitochondrial OXPHOS complex protein degradation (likely due to impaired mitophagy) and outer mitochondrial membrane protein degradation (likely due to decreased ubiquitination and proteasomal degradation) after APAP treatment compared with WT, PINK1 KO and Parkin KO mice. Impaired mitophagy in APAP-treated PINK1 and Parkin DKO mice may also lead to dysfunctional mitochondrial respiration in mouse livers despite an overall increase in the OXPHOS complexes.

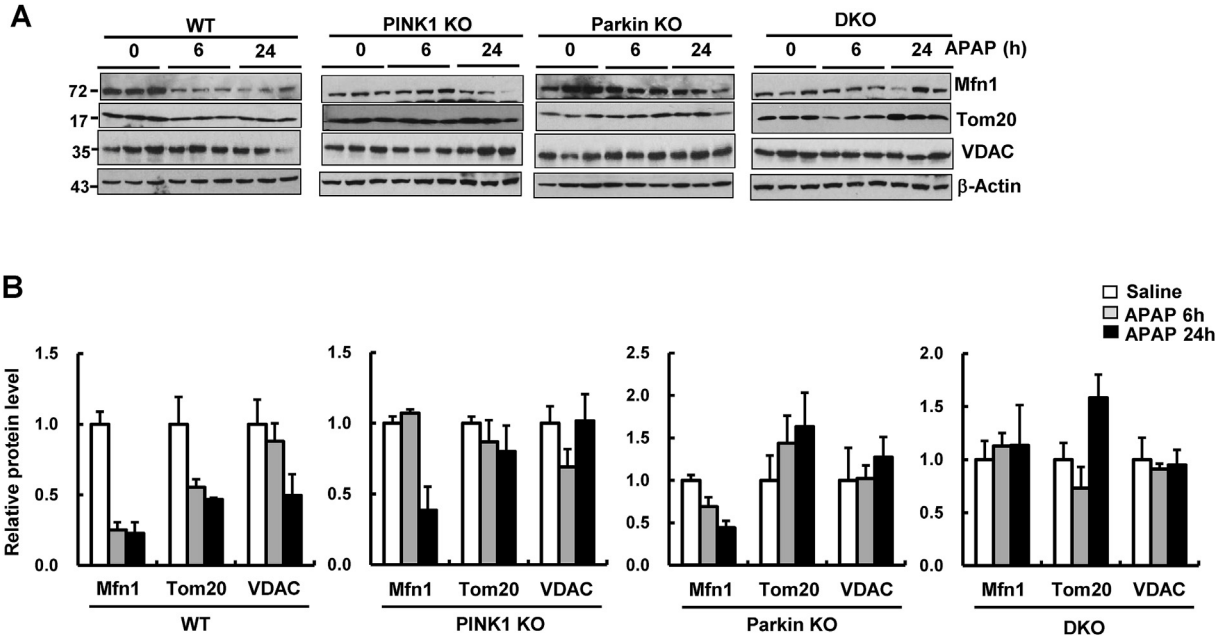

Fig. 8. APAP treatment decreased outer mitochondrial membrane protein Mfn1 and Tom20 in WT but not in PINK1 and Parkin DKO mice. Male WT, Parkin KO, PINK1 KO, PINK1 and Parkin DKO (C57BL/6J) mice were treated with saline or APAP (500 mg/kg, i.p.) for 6 and 24 h. (**A**) Total liver lysates were subjected to western blot analysis. (**B**) Densitometry analysis of (**A**). Data are means ± SE (n = 3).

3.6. Increased JNK activation in the early phase but not late phase of APAP-induced liver injury in PINK1 and Parkin DKO mice

We found the levels of phosphorylated JNK (pJNK) increased at 6 h but decreased at 24 h after APAP treatment in WT and DKO mice. In contrast, the levels of pJNK increased at 6 h and sustained at 24 h after APAP treatment in PINK1 KO mice (Fig. 9A). When liver lysates from APAP-treated mice with different genotype were placed on the same blot, it showed higher levels of pJNK in PINK1 KO and DKO mice compared to WT or Parkin KO mice after APAP treatment for 6 h. Interestingly, the levels of pJNK remained remarkably higher in PINK1 KO mice but were almost undetectable in WT, Parkin KO, PINK1 and Parkin DKO mice after APAP treatment for 24 h (Fig. 9B). These data indicate that the levels of JNK activation may be higher in PINK1 and Parkin DKO mice at the early phase but not the late phase after APAP treatment. In contrast, the levels of JNK activation are sustained at both the early and late phase of APAP treatment in PINK1 KO mice (see Fig. 9B).

4. Discussion

We previously reported that Parkin differentially regulates APAP-induced mitophagy [8]. The role of Parkin in APAP-induced liver injury depends on whether Parkin is chronically deleted or acutely knocked down in mouse livers. We found that mitophagy still occurred in hepatocytes of Parkin KO mice after APAP treatment, but acute knockdown of Parkin markedly decreased APAP-induced mitophagy [8]. These observations have led us to speculate that Parkin KO mice may have adapted and use alternative Parkin-independent compensatory pathways to trigger mitophagy. Under acute knockdown conditions, the adaptive response may not have been initiated. Parkin KO mice are viable and only have mild and inconsistent mitochondrial phenotypes [8,32,33]. All these earlier studies together with ours suggest that redundant proteins may exist to compensate for the loss of Parkin. However, such adaptive compensatory mechanisms are largely unknown and have not been explored in APAP-induced mitophagy and liver injury.

Several other ubiquitin E3 ligases have been reported that can also trigger mitophagy in addition to Parkin. In a high-content, image-based, genome-wide small interfering RNA screen, SMURF1, a C2-domain containing protein that has E3 ubiquitin ligase activity, induces mitophagy in cultured cells. An increased number of damaged mitochondria were found in the heart, brain and liver of SMURF1 KO mice [34]. During the elimination of paternal mitochondria in mouse embryos, it was found that Parkin and MUL1, another E3 ubiquitin ligase, have redundant roles in mitophagy [19]. Parkin KO cells have normal mitophagy but further knockdown of MUL1 abolished mitophagy in Parkin KO cells [19]. Compared with either WT, PINK1 or Parkin KO mice, we found that the levels of mitochondrial ubiquitination markedly decreased in PINK1 and Parkin DKO mice. Moreover, after APAP treatment of PINK1 and Parkin DKO mice, the levels of mitochondrial ubiquitination did not increase compared with saline-treated mice. These data suggest that PINK1 and Parkin could be the dominate pathway in regulating mitochondrial ubiquitination and mitophagy in mouse livers after APAP. Other E3 ligases such as SMURF1 and MUL1 may only play a minor role in APAP-induced ubiquitination of mitochondria and mitophagy. However, whether the residual mitochondrial ubiquitination in PINK1 and Parkin DKO mice is mediated by SMURF1 and MUL1 remains to be studied in the future.

One of the key steps in mitophagy is the selective recognition of damaged mitochondria by autophagosomes. The selective process for mitochondria is mediated by mitophagy receptor proteins. Generally, a mitophagy receptor must be present on mitochondria and can directly interact with proteins of the autophagy machinery such as LC3 via the LIR (LC3 interacting region) [11,35]. Several mitophagy receptor proteins such as Nix, Bnip3 and Fundc1 may directly recruit the autophagy machinery to mitochondria independent of PINK1 and Parkin. In contrast, p62 normally resides at cytosol but can translocate to ubiquitinated mitochondria via direct binding with ubiquitin followed by the recruitment of autophagosomes through direct interaction with LC3 [19,36,37]. Using EM and confocal microscopy of the mitophagy reporter protein Cox8-GFP-mCherry, we found that there were still some basal levels of mitophagy in PINK1 and Parkin DKO mouse livers (albeit mitophagy in DKO mouse livers did not further increase after APAP), suggesting that some of the mitophagy receptor proteins could be responsible for the basal mitophagy in PINK1 and Parkin DKO

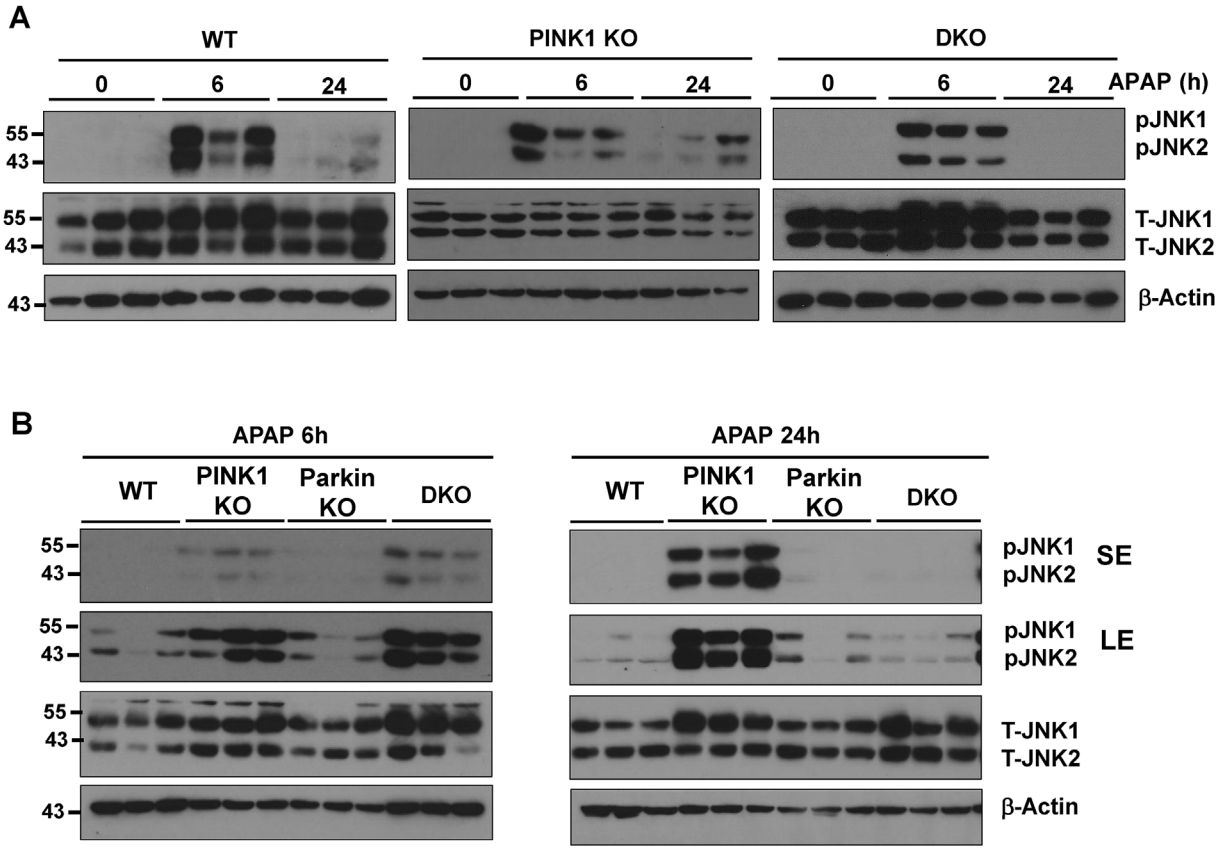

Fig. 9. Increased JNK activation in the early phase but not late phase of APAP-induced liver injury in PINK1 and Parkin DKO mice. Male WT, Parkin KO, PINK1 KO, PINK1 and Parkin DKO (C57BL/6J) mice were treated with saline or APAP (500 mg/kg, i.p.) for 6 and 24 h. (**A**) Total liver lysates were subjected to western blot analysis. (**B**) Male WT, Parkin KO, PINK1 KO, PINK1 and Parkin DKO mice were treated with APAP (500 mg/kg, i.p.) for 6 and 24 h. Total liver lysates were subjected to western blot analysis. SE: Short exposure. LE: Longer exposure.

hepatocytes independent of PINK1 and Parkin. While it is beyond the scope of this report, further studies are needed to further examine the role of these receptor proteins in APAP-induced mitophagy and liver injury. Recently, formation of mitochondrial-derived vesicles (MDVs), a novel mitochondrial degradation pathway independent of mitophagy, has been proposed [11,38,39]. MDVs are single membrane vesicles that bud off damaged mitochondria, which contain some oxidized mitochondrial proteins and fuse with endosomes and lysosomes for degradation. Future studies are needed to determine whether some of the basal mitochondrial turn over in PINK1 and Parkin DKO mice that we observed are mediated by MDVs or not.

What are the advantages and disadvantages of using Ad-Cox8-GFP-mCherry to monitor mitophagy in mouse livers? It should be noted that a transgenic mouse line of Mito-QC, a tandem mCherry-GFP tag fused to the mitochondrial targeting sequence of the outer mitochondrial membrane protein, has been recently established to monitor mitophagy *in vivo* [40]. However, as discussed above, most outer mitochondrial membrane proteins are degraded by the ubiquitin proteasome system during mitophagy whereas inner mitochondrial membrane proteins are more specifically degraded by mitophagy [11]. Therefore, the use of Cox8-GFP-mCherry may be more specific to monitor mitophagy in mouse livers. Another advantage of using Ad-Cox8-GFP-mCherry is that one can directly overexpress Cox8-GFP-mCherry in mouse livers of different strains to avoid the time-consuming cross-breeding. However, there are also some disadvantages and limitations of using Ad-Cox8-GFP-mCherry to monitor mitophagy. The expression levels of Cox8-GFP-mCherry vary in different cells due to the different amount of adenovirus each cell received in particularly in liver tissues. Moreover, adenovirus may cause some inflammatory response in the liver, which may affect the sensitivity to different drugs including APAP.

One of the novel perspectives in our present study is that we determined APAP-induced liver injury and mitophagy in PINK1 KO and PINK1 and Parkin DKO mice. It has been thought that PINK1 acts upstream of Parkin as a linear pathway, in which PINK1 phosphorylates both Parkin and ubiquitin to recruit Parkin to mitochondria for mitochondrial outer membrane protein ubiquitination and mitophagy [14,16,21]. We found that the phenotypes in PINK1 KO mice after APAP treatment were largely similar to the Parkin KO mice. Both Parkin KO and PINK1 KO showed decreased levels of serum of ALT at 6 h with better survival after APAP treatment, although PINK1 KO mice showed higher levels of serum ALT at 24 h after APAP. APAP treatment increased mitochondrial Parkin translocation in WT mice, which was markedly blunted in PINK1 KO mice. These data suggest that PINK1 and Parkin likely also work in a linear pathway in mouse livers and PINK1 acts upstream of Parkin, which is similar to those findings in *Drosophila melanogaster* and mammalian cell culture studies [14,20]. However, compared with either WT, PINK1 KO or Parkin KO mice, the levels of mitochondrial ubiquitination and mitophagy decreased dramatically in PINK1 and Parkin DKO mice after APAP treatment, suggesting that it is possible that Parkin and PINK1 may also reciprocally compensate for each other in addition to working in the linear pathway in mouse livers. It should be noted that both PINK1 and Parkin have other functions including regulating cell survival and proliferation in addition to regulating mitophagy [41,42]. In addition, the whole body PINK1 KO and Parkin KO mice may already have developed other adaptive responses that influence the APAP-induced liver injury and mortality independent of mitophagy. Future studies are needed to identify these mitophagy-independent functions of loss of PINK1 or Parkin, which contribute to the improved survival of APAP-treated mice.

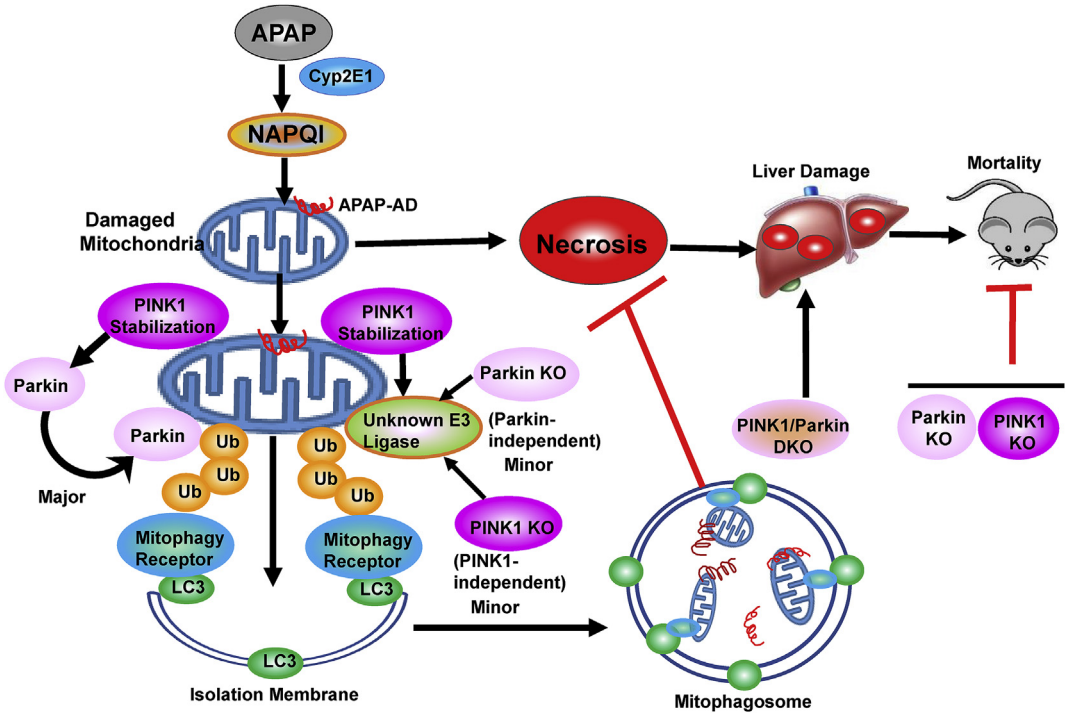

Fig. 10. A proposed model for PINK1-Parkin-mediated mitophagy in APAP-induced liver injury. In hepatocytes, APAP is first metabolized through the Cyp2E1 and generates reactive metabolites NAPQI, which bind to cellular and mitochondrial proteins to form APAP-adducts (APAP-AD) that damage mitochondria. Damaged mitochondria can lead to necrotic cell death and subsequent liver injury. PINK1 is stabilized on damaged mitochondria and further recruit Parkin to mitochondrial to induce ubiquitination of mitochondria, which plays a major role in APAP-induced mitochondrial ubiquitination and mitophagy. In the absence of Parkin, PINK1 can trigger Parkin-independent mitophagy likely via activating unknown E3 ligase on mitochondria to induce ubiquitination of mitochondria. In the absence of PINK1, some other unknown E3 ligase could also be recruited to mitochondria to induce ubiquitination of mitochondria independent of PINK1. Both the PINK1-independent and Parkin-independent mitophagy plays a minor role in APAP-induced mitophagy. The autophagy receptor protein such as p62 is recruited to damaged ubiquitinated mitochondria that further recruits LC3 positive autophagosomes for selective mitophagy, which protects against APAP-induced necrosis by removing damaged mitochondria. PINK1 KO and Parkin KO mice have improved survival rate after APAP treatment likely via the mitophagy-independent functions. Double deletion of PINK1 and Parkin in mice decreases mitophagy, exacerbates APAP-induced liver injury and mortality.

How does PINK1-Parkin-mediated mitophagy protect against APAP-induced liver injury? Mitochondria damage has been well recognized as a central key mechanism contributing to APAP-induced necrosis by releasing mitochondrial cell death factors such as cytochrome *c*, AIF and endonuclease G as well as increasing oxidative stress [5,6]. Thus, it is easily conceivable that mitophagy protects against APAP-induced liver injury by simply removing these damaged mitochondria in hepatocytes. We previously demonstrated that APAP induces unique zonated changes in mouse livers due to different metabolic functions/activities in these liver zone areas [43]. APAP-induced necrosis mainly occurs in the central vein areas because of the enrichment of Cyp2e1 in these areas. APAP-induced mitophagy occurs adjacent to the necrosis areas likely serves as a protective barrier to restrict the expansion of necrosis in the liver. In contrast, increased hepatocyte proliferation and mitochondria biogenesis occur in the outer layer of the hepatocytes that are adjacent to the portal vein area [43,44]. Because of these unique different zone changes after APAP, one has to be cautious with the data interpretation for mitochondrial changes when using isolated mitochondria from the whole liver. This probably explains why we did not see significant impaired mitochondrial OCR in WT, PINK1 KO and Parkin KO mice after APAP treatment. However, we did observe decreased levels of mitochondrial OCR in isolated mitochondria from APAP-treated PINK1 and Parkin DKO mice. These data may suggest that impaired mitochondrial functions in APAP-treated PINK1 and DKO mice, which could be either due to impaired mitophagy or decreased mitochondrial biogenesis or both. Future work to use microdissection to isolate mitochondrial directly from different liver zone areas would help to clarify the zonated changes of mitochondria and their contributions in APAP-induced liver injury.

In conclusion, we found that Parkin and PINK1 may reciprocally compensate for each other in regulating mitophagy in addition to working in a linear pathway in regulating mitophagy in APAP-treated mouse livers. Double deletion of Parkin and PINK1 severely impaired mitophagy in mouse livers resulting in exacerbated liver injury and mortality after APAP overdose. The molecular and cellular events of PINK1-Parkin-mediated mitophagy in APAP-induced liver injury is summarized in Fig. 10.

Contributions of the authors

H.W., H.M.N, X.C., Y.A.R., H.C., S.W., P.K., and W.X.D performed experiments. W.X.D, D.X.C., R.D. and H.J. conceived the idea and supervised the project. H.W., W.X.D., R.D., and H.J. wrote the manuscript. Everyone read this manuscript and approved for submission. There is no conflict of interests to claim for all the authors.

Acknowledgements

This research was supported in part by NIH R01 AA 020518, R01 DK 102142, U01 AA 024733 (W.X.D), P20 GM 103549 and P30 GM 118247 (H.J.). We wish to acknowledge the University of Kansas Medical Center Electron Microscopy Research Lab facility for assistance with the TEM. The EMRL is supported in part, by NIH COBRE grant 9P20GM104936. The JEOL JEM-1400 TEM used in the study was purchased with funds from NIH grant S10RR027564.

References

[1] S.D. Nelson, Molecular mechanisms of the hepatotoxicity caused by acetaminophen, Semin. Liver Dis. 10 (1990) 267–278.
[2] A.M. Larson, Acetaminophen hepatotoxicity, Clin. Liver Dis. 11 (2007) 525–548 vi.
[3] M.R. McGill, H. Jaeschke, Metabolism and disposition of acetaminophen: recent advances in relation to hepatotoxicity and diagnosis, Pharm . Res. 30 (2013) 2174–2187.
[4] J.A. Hinson, D.W. Roberts, L.P. James, Mechanisms of acetaminophen-induced liver necrosis, Handb. Exp. Pharmacol. (2010) 369–405.
[5] A. Ramachandran, H. Jaeschke, Acetaminophen toxicity: novel insights into mechanisms and future perspectives, Gene Expr. 18 (2018) 19–30.
[6] X. Chao, H. Wang, H. Jaeschke, W.X. Ding, Role and mechanisms of autophagy in acetaminophen-induced liver injury, Liver Int. 38 (2018) 1363–1374.
[7] H.M. Ni, M.R. McGill, X. Chao, K. Du, J.A. Williams, Y. Xie, et al., Removal of acetaminophen protein adducts by autophagy protects against acetaminophen-induced liver injury in mice, J. Hepatol. 65 (2016) 354–362.
[8] J.A. Williams, H.M. Ni, A. Haynes, S. Manley, Y. Li, H. Jaeschke, et al., Chronic deletion and acute knockdown of parkin have differential responses to acetaminophen-induced mitophagy and liver injury in mice, J. Biol. Chem. 290 (2015) 10934–10946.
[9] H.M. Ni, A. Bockus, N. Boggess, H. Jaeschke, W.X. Ding, Activation of autophagy protects against acetaminophen-induced hepatotoxicity, Hepatology 55 (2012) 222–232.
[10] H.M. Ni, J.A. Williams, W.X. Ding, Mitochondrial dynamics and mitochondrial quality control, Redox Biol. 4 (2015) 6–13.
[11] J.A. Williams, W.X. Ding, Mechanisms, pathophysiological roles and methods for analyzing mitophagy - recent insights, Biol. Chem. 399 (2018) 147–178.
[12] K. Yamano, R.J. Youle, PINK1 is degraded through the N-end rule pathway, Autophagy 9 (2013) 1758–1769.
[13] D.P. Narendra, S.M. Jin, A. Tanaka, D.F. Suen, C.A. Gautier, J. Shen, et al., PINK1 is selectively stabilized on impaired mitochondria to activate Parkin, PLoS Biol. 8 (2010) e1000298.
[14] N. Matsuda, S. Sato, K. Shiba, K. Okatsu, K. Saisho, C.A. Gautier, et al., PINK1 stabilized by mitochondrial depolarization recruits Parkin to damaged mitochondria and activates latent Parkin for mitophagy, J. Cell Biol. 189 (2010) 211–221.
[15] C. Vives-Bauza, C. Zhou, Y. Huang, M. Cui, R.L. de Vries, J. Kim, et al., PINK1-dependent recruitment of Parkin to mitochondria in mitophagy, Proc. Natl. Acad. Sci. U. S. A 107 (2010) 378–383.
[16] F. Koyano, K. Okatsu, H. Kosako, Y. Tamura, E. Go, M. Kimura, et al., Ubiquitin is phosphorylated by PINK1 to activate parkin, Nature 510 (2014) 162–166.
[17] L.M. Wang, Y.L. Cho, Y.C. Tang, J.G. Wang, J.E. Park, Y.J. Wu, et al., PTEN-L is a novel protein phosphatase for ubiquitin dephosphorylation to inhibit PINK1-Parkin-mediated mitophagy, Cell Res. 28 (2018) 787–802.
[18] S. Pickles, P. Vigie, R.J. Youle, Mitophagy and quality control mechanisms in mitochondrial maintenance, Curr. Biol. CB 28 (2018) R170–R185.
[19] R. Rojansky, M.Y. Cha, D.C. Chan, Elimination of paternal mitochondria in mouse embryos occurs through autophagic degradation dependent on PARKIN and MUL1, eLife 5 (2016).
[20] I.E. Clark, M.W. Dodson, C. Jiang, J.H. Cao, J.R. Huh, J.H. Seol, et al., Drosophila pink1 is required for mitochondrial function and interacts genetically with parkin, Nature 441 (2006) 1162–1166.
[21] M. Lazarou, D.A. Sliter, L.A. Kane, S.A. Sarraf, C. Wang, J.L. Burman, et al., The ubiquitin kinase PINK1 recruits autophagy receptors to induce mitophagy, Nature 524 (2015) 309–314.
[22] P.M. Ryan, M. Bourdi, M.C. Korrapati, W.R. Proctor, R.A. Vasquez, S.B. Yee, et al., Endogenous interleukin-4 regulates glutathione synthesis following acetaminophen-induced liver injury in mice, Chem. Res. Toxicol. 25 (2012) 83–93.
[23] H.M. Ni, B.L. Woolbright, J. Williams, B. Copple, W. Cui, J.P. Luyendyk, et al., Nrf2 promotes the development of fibrosis and tumorigenesis in mice with defective hepatic autophagy, J. Hepatol. 61 (2014) 617–625.
[24] H.M. Ni, K. Du, M. You, W.X. Ding, Critical role of FoxO3a in alcohol-induced autophagy and hepatotoxicity, Am. J. Pathol. 183 (2013) 1815–1825.
[25] W.X. Ding, H.M. Ni, D. DiFrancesca, D.B. Stolz, X.M. Yin, Bid-dependent generation of oxygen radicals promotes death receptor activation-induced apoptosis in murine hepatocytes, Hepatology 40 (2004) 403–413.
[26] H. Jaeschke, J.R. Mitchell, Use of Isolated Perfused Organs in Hypoxia and Ischemia/reperfusion Oxidant Stress, (1990), pp. 752–759.
[27] H. Jaeschke, Glutathione disulfide formation and oxidant stress during acetaminophen-induced hepatotoxicity in mice in vivo: the protective effect of allopurinol, J. Pharmacol. Exp. Therapeut. 255 (1990) 935–941.
[28] X. Chao, S. Wang, K. Zhao, Y. Li, J.A. Williams, T. Li, et al., Impaired TFEB-mediated lysosome biogenesis and autophagy promote chronic ethanol-induced liver injury and steatosis in mice, Gastroenterology 155 (2018) 865–879 e812.
[29] W.X. Ding, X.M. Yin, Mitophagy: mechanisms, pathophysiological roles, and analysis, Biol. Chem. 393 (2012) 547–564.
[30] D.J. Klionsky, F.C. Abdalla, H. Abeliovich, R.T. Abraham, A. Acevedo-Arozena, K. Adeli, et al., Guidelines for the use and interpretation of assays for monitoring autophagy, Autophagy 8 (2012) 445–544.
[31] N.C. Chan, A.M. Salazar, A.H. Pham, M.J. Sweredoski, N.J. Kolawa, R.L. Graham, et al., Broad activation of the ubiquitin-proteasome system by Parkin is critical for mitophagy, Hum. Mol. Genet. 20 (2011) 1726–1737.
[32] J.A. Williams, H.M. Ni, Y. Ding, W.X. Ding, Parkin regulates mitophagy and mitochondrial function to protect against alcohol-induced liver injury and steatosis in mice, Am. J. Physiol. Gastrointest. Liver Physiol. 309 (2015) G324–G340.
[33] J.J. Palacino, D. Sagi, M.S. Goldberg, S. Krauss, C. Motz, M. Wacker, et al., Mitochondrial dysfunction and oxidative damage in parkin-deficient mice, J. Biol. Chem. 279 (2004) 18614–18622.
[34] A. Orvedahl, R. Sumpter Jr., G. Xiao, A. Ng, Z. Zou, Y. Tang, et al., Image-based genome-wide siRNA screen identifies selective autophagy factors, Nature 480 (2011) 113–117.
[35] L. Liu, K. Sakakibara, Q. Chen, K. Okamoto, Receptor-mediated mitophagy in yeast and mammalian systems, Cell Res. 24 (2014) 787–795.
[36] W.X. Ding, H.M. Ni, M. Li, Y. Liao, X. Chen, D.B. Stolz, et al., Nix is critical to two distinct phases of mitophagy, reactive oxygen species-mediated autophagy induction and Parkin-ubiquitin-p62-mediated mitochondrial priming, J. Biol. Chem. 285 (2010) 27879–27890.
[37] Z. Zhong, A. Umemura, E. Sanchez-Lopez, S. Liang, S. Shalapour, J. Wong, et al., NF-kappaB restricts inflammasome activation via elimination of damaged mitochondria, Cell 164 (2016) 896–910.
[38] V. Soubannier, G.L. McLelland, R. Zunino, E. Braschi, P. Rippstein, E.A. Fon, et al., A vesicular transport pathway shuttles cargo from mitochondria to lysosomes, Curr. Biol. CB 22 (2012) 135–141.
[39] G.L. McLelland, V. Soubannier, C.X. Chen, H.M. McBride, E.A. Fon, Parkin and PINK1 function in a vesicular trafficking pathway regulating mitochondrial quality control, EMBO J. 33 (2014) 282–295.
[40] T.G. McWilliams, A.R. Prescott, G.F. Allen, J. Tamjar, M.J. Munson, C. Thomson, et al., mito-QC illuminates mitophagy and mitochondrial architecture in vivo, J. Cell Biol. 214 (2016) 333–345.
[41] C.H. O'Flanagan, C. O'Neill, PINK1 signalling in cancer biology, Biochim. Biophys. Acta 1846 (2014) 590–598.
[42] L. Xu, D.C. Lin, D. Yin, H.P. Koeffler, An emerging role of PARK2 in cancer, J. Mol. Med. 92 (2014) 31–42.
[43] H.M. Ni, J.A. Williams, H. Jaeschke, W.X. Ding, Zonated induction of autophagy and mitochondrial spheroids limits acetaminophen-induced necrosis in the liver, Redox Biol. 1 (2013) 427–432.
[44] K. Du, A. Ramachandran, M.R. McGill, A. Mansouri, T. Asselah, A. Farhood, et al., Induction of mitochondrial biogenesis protects against acetaminophen hepatotoxicity, Food Chem. Toxicol. Int. J. Publ. Br. Ind. Biol. Res. Assoc. 108 (2017) 339–350.